Am J Transl Res 2026;18(1):771-787
www.ajtr.org /ISSN:1943-8141/AJTR0169785

Original Article

Fasudil improves neutrophilic asthma by influencing M1 macrophage polarization and the expression of the NF-κB/TLR-2/RPS3 pathway

Shang-De Guo[1,2], Chun-Yun Liu[1], Rong Liu[1], Yi-Ping Zhang[1], Li-Yun Zuo[1], Cai-Yun Cui[2,3], Jing Cheng[2,3], Tao Lin[2,3]

[1]Institute of Respiratory and Occupational Diseases, Shanxi Datong University, Datong, Shanxi, China; [2]Shanxi Datong University First Affiliated Hospital, Respiratory and Critical Care Department, Datong, Shanxi, China; [3]Department of Respiratory and Critical Care Medicine The Fifth People's Hospital of Datong, Datong, Shanxi, China

Received November 4, 2025; Accepted December 30, 2025; Epub January 15, 2026; Published January 30, 2026

Abstract: Neutrophilic asthma (NA), an asthma subtype characterized by neutrophil-predominant airway inflammation, lacks effective targeted therapies. Fasudil, with documented anti-oxidative and anti-inflammatory effects in airway models, was evaluated for its therapeutic efficacy and underlying mechanisms in an NA model. BALB/C mice were randomized into an NA group, a dexamethasone intervention group (DI, 1 mg/kg), and a Fasudil intervention group (FI, 40 mg/kg). Asthma was induced by intraperitoneal ovalbumin (OVA) sensitization and intranasal lipopolysaccharide (LPS) infusion, followed by OVA aerosol challenge. Dexamethasone or Fasudil was administered intraperitoneally 1 h before each aerosol exposure. Outcome assessments included behavioral stress responses, airway hyperresponsiveness (AHR), total and differential bronchoalveolar lavage fluid (BALF) cell counts, lung histopathology, and macrophage contents, inflammatory mediators and cytokine expression. Transcriptome sequencing with bioinformatic analysis was performed. Blood samples from NA patients were collected for clinical validation. Both dexamethasone and Fasudil significantly alleviated behavioral stress responses, improved asthma symptoms, and reduced levels of interleukin-6 (IL-6), IL-1β, tumor necrosis factor alpha (TNF-α), inducible nitric oxide synthase (iNOS), and IL-12. Additionally, treatment also decreased the expression of phosphorylated nuclear factor kappa B (p-NF-κB), toll-like receptor 2 (TLR-2) and ribosomal protein S3 (RPS3), as well as total BALF cells and neutrophil-to-macrophage ratios. Fasudil outperformed dexamethasone in relieving respiratory distress, inhibiting macrophage polarization, suppressing the NF-κB/TLR-2/RPS3 pathway, and improving AHR in a time-dependent manner. Key hub genes including ROCK2, S100A8, S100A9, Mmp9, and CXCL2 were identified to mediate Fasudil's anti-inflammatory effects. Clinical data showed elevated S100A8 and CXCL2 levels in NA patients, which positively correlated with sputum neutrophil percentages. Fasudil ameliorates NA via regulating M1 macrophage polarization, inhibiting the NF-κB/TLR-2/RPS3 pathway, and reducing pro-inflammatory cytokines, with S100A8/A9 and CXCL2 as potential biomarkers. These findings support Fasudil as a promising NA therapy, warranting further clinical translational research.

Keywords: Fasudil, neutrophilic asthma, M1 macrophage, signaling pathway

Introduction

Bronchial asthma (commonly referred to as asthma) is a chronic respiratory disorder characterized by persistent airway inflammation, heightened airway responsiveness to diverse stimuli, and structural remodeling of the airways. Clinically, it manifests as recurrent wheezing, dyspnea, coughing, chest tightness, or shortness of breath, aggravated at night or early in the morning. In recent years, with accelerating industrialization and urbanization, along with aggravated environmental pollution, climate change and other factors, the global incidence of asthma is on the rise, resulting in an increasing disease-related, social, and economic burden. Asthma attacks substantially impair patients' daily activities and work, and are

https://doi.org/10.62347/MVRX1911

associated with heightened risk of disability and mortality. According to estimates from the World Health Organization (WHO), asthma affects approximately 15 million people globally each year, accounting for about 1% of the global disease burden with an estimated 250,000 asthma-related deaths annually [1-3]. Asthma has become one of the major chronic diseases that seriously threaten human health.

"Overall asthma control" aims to achieve effective symptom control, maintain normal daily activities, preserve lung function, prevent acute exacerbations, minimize adverse reactions related to asthma medications, and reduce asthma-related deaths [4]. Corticosteroids and β2 receptor agonists are the current first-line drugs for asthma. Although these agents are effective in relieving acute exacerbations and shortening the disease course in severe asthma, some patients remain poorly controlled. In particular, long-term and excessive use of glucocorticoids is often associated with increased risk of adverse effects and unfavorable outcomes [5, 6], a condition referred to as "glucocorticoid-resistant asthma". Therefore, there is an urgent need to develop effective therapeutic drugs or prevention strategies with fewer side effects.

Although the precise etiology of asthma remains unclear, airway inflammation is a fundamental pathophysiological alteration that leads to airway remodeling and hyperresponsiveness. Many inflammatory cells, including mast cells, macrophages, and granulocytes, are involved in this immunologically mediated airway inflammation. Of these, macrophages are thought to play a pivotal role in regulating immune responses [7, 8]. Macrophages are highly plastic and multifunctional, exhibiting varying phenotypic and functional states in response to changes in the microenvironment [9]. M1 macrophages are a classically activated phenotype, which produce pro-inflammatory factors and exert cytotoxic effects through various reactive nitrogen species and oxygen species, causing inflammatory tissue damage. M1 macrophages can mediate T-cell effector responses through antigen presentation, accompanied by the secretion of pro-inflammatory cytokines including IL-12 and IL-23, thereby promoting T1 and T17 cell differentiation and neutrophil-driven inflammation [10-12]. Studies have shown that, compared with eosinophilic asthma, M1 macrophages are more prevalent in the sputum of non-eosinophilic asthma patients, and their percentage is positively correlated with that of neutrophils, indicating a close association between M1 macrophage polarization and airway neutrophilia in asthma patients. In contrast, M2 macrophages are selectively activated and predominantly secrete anti-inflammatory cytokines, contributing to the suppression of inflammatory immune responses and tissue repair [13, 14].

Rho kinase (ROCK), discovered in the past decade, participates in various cellular activities. There are two subtypes of ROCK, ROCK-I and ROCK-II, with ROCK-I being more abundantly expressed in lung tissue. Various stimuli, including hormones, growth factors, extracellular matrix components, and mechanical stimulation, can activate ROCK signaling, leading to diverse biological effects such as cytoskeleton organization, cell migration and proliferation, cell adhesion, smooth muscle contraction, and regulation of cell growth and apoptosis [15, 16]. These physiological responses mediated by the ROCK signaling pathway may be associated with the pathophysiological features of asthma, such as airflow restriction, airway hyperresponsiveness (AHR), and airway remodeling. Studies have shown that Fasudil, a selective ROCK inhibitor, can reduce eosinophil infiltration in bronchoalveolar lavage fluid (BALF), inhibit endotracheal cell adhesion and oxygen radicals generation, and attenuate airway hyperreactivity [17, 18]. Therefore, this research established a neutrophilic asthma (NA) model to explore the therapeutic efficacy and potential molecular targets of Fasudil in treating asthma.

Materials and methods

Animals

Female BALB/C mice (18-22 g, 6-8 weeks old) were obtained from Beijing Huafukang Bioscience Co., Ltd. (Beijing, China) and reared under specific pathogen-free conditions in a temperature-controlled chamber (25 ± 2°C). Prior to commencement, this study was approved by the Animal Ethics Committee of Shanxi Datong University. All subsequent experimental procedures were carried out in compli-

ance with the National Institutes of Health Guide for the Care and Use of Laboratory Animals.

Establishment of the asthma model

Mice were randomly assigned into three groups (n = 25 per group) using a random number table: neutrophilic asthma (NA) group, dexamethasone intervention (DI) group, and Fasudil intervention (FI) group.

NA group: On days 0, 7, and 14, mice were anesthetized with ether and given 10 μg of lipopolysaccharide (LPS) (Sigma, St Louis, USA) via intranasal instillation, alternating nostrils for each administration. Simultaneously, mice received an intraperitoneal injection of 200 μl of sensitizing solution containing 100 μg ovalbumin (OVA) (Sigma) and 2 mg $Al(OH)_3$ (Thermo Fisher Scientfc, Waltham, USA). Starting from day 21, mice were placed in a self-made nebulization chamber and stimulated by atomizing inhalation with 5% OVA solution (15 ml) for 30 minutes per day for 2 weeks. Normal saline (20 ml) was given intraperitoneally 1 hour before each atomization.

DI group: Mice underwent the same sensitization and stimulation as the NA group. Dexamethasone (1 mg/kg/day) (Guangzhou Baiyunshan Tianxin Pharmaceutical Co., Ltd, Guangzhou, China) was given intraperitoneally 1 hour before each atomization.

FI group: Mice underwent the same sensitization and stimulation as the NA group. Fasudil (40 mg/kg/day) (Tianjin Chase Sun Pharmaceutical Co., Tianjin, China) was administered intraperitoneally 1 hour before each atomization.

To objectively evaluate the severity of stress responses in asthmatic mice, a systematic scoring system was developed based on observable behavioral symptoms. The scoring criteria were as follows:

(1) Breathing pattern (0-3 points): 0: Normal breathing, 1: Mild respiratory deepening, 2: Obvious deepened abdominal breathing, 3: Severe dyspnea.

(2) Behavioral activity (0-3 points): 0: Normal activity, 1: Mild restlessness, 2: Frequent scratching of the ears and cheeks, 3: Head retraction and back arching.

(3) Neurological symptoms (0-2 points): 0: No abnormalities, 1: Mild abdominal muscle twitching, 2: Severe convulsions with incontinence.

(4) Overall condition (0-2 points): 0: Good condition, 1: Mild lethargy, 2: Severe lethargy.

All animal experiments were conducted in accordance with protocols approved by the Animal Ethics Committee (Approval No. 2012046). At the experimental endpoint, euthanasia was performed under deep anesthesia induced by pentobarbital sodium. Following the induction of surgical anesthesia, a terminal bronchoalveolar lavage procedure was conducted to collect samples. To ensure death, euthanasia was further confirmed by exsanguination or cervical dislocation while animals remained fully anesthetized, followed by verification of cessation of vital signs.

The maximum total score was 10 points. Behavioral assessments were conducted by two independent observers blinded to the treatment groups at days 21, 27, and 34 during the OVA challenge period. The average score from both observers was used for statistical analysis.

Dynamic assessment of AHR and inflammation at multiple time points

To evaluate the longitudinal therapeutic effects of Fasudil, AHR and inflammatory cell profiles were assessed at days 21, 27, and 34 throughout the OVA challenge phase. At each timepoint, an independent subset of mice (n = 5 per group per time point) was randomly chosen for AHR measurement, followed immediately by terminal sample collection.

AHR was quantified non-invasively by recording the enhanced pause (Penh) parameter using a Buxco whole-body plethysmograph. Mice were first placed in the plethysmography chambers and allowed to acclimate for 10 minutes. Baseline Penh readings were obtained after exposure to an aerosol of sterile PBS for 3 minutes. Subsequently, mice were challenged with sequentially increasing concentrations of aerosolized methacholine (MCh; 0, 3.125, 6.25, 12.5, and 25 mg/mL in PBS). The Penh value was recorded and averaged over a 3-minute period immediately following each 3-minute

nebulization cycle. All AHR data were expressed in dimensionless Penh units. Sample collection was initiated immediately after the final MCh measurement.

Directly after the AHR assessment at each scheduled time point, deep anesthesia was induced in mice via an intraperitoneal injection of 2% pentobarbital (40 mg/kg, Sigma). A tracheal cannula was then inserted after the trachea was surgically exposed. Lung lavage was performed using three sequential instillations of 0.4 mL ice-cold, sterile PBS, yielding a total lavage volume of 1.2 mL. The collected BALF was centrifuged at 2,000 rpm for 5 min at 4°C. The supernatant was aliquoted and cryopreserved at -80°C for subsequent analysis, while the cell pellet was resuspended in 100 μL of PBS for total cell counting using a hemocytometer. For differential analysis, cytospin cell preparations were stained with Wright-Giemsa, and a minimum of 200 cells per sample were identified and counted based on standard morphological characteristics under light microscopy to determine the proportions of neutrophils (NEU%), macrophages (Mφ%), lymphocytes, and eosinophils. NEU% and Mφ% served as the primary endpoints for this analysis.

Histopathological evaluation of lung tissue

Five mice were randomly selected from each group and anesthetized. The right lung lobes were aseptically excised, fixed in paraformaldehyde, embedded in paraffin, and sectioned for histological analysis by hematoxylin eosin staining (H&E) staining. The staining procedure included xylene dewaxing, rehydration through a graded alcohol series, hematoxylin (Beyotime Institute of Biotechnology, Shanghai, China) staining, differentiation in hydrochloric acid-alcohol, eosin (Beyotime) counterstaining, dehydration via graded ethanol, xylene clearing, and final mounting with neutral resin. The morphology and structure of lung tissue, airway epithelial damage, and inflammatory cell infiltration around the trachea were observed under an optical microscope. A semi-quantitative method was used to score the degree of inflammatory cell infiltration around the bronchioles, as previously described [19]. Scores were assigned as follows: 0, no inflammatory cell invasion; 2, a single layer of peribronchiolar inflammatory cell infiltration; 3, two to four layers; and 4, more than four layers of inflammatory cell infiltration around the bronchioles.

Flow cytometry assay

Under aseptic conditions, the left lungs of the five mice were harvested and washed with precooled PBS. Lung tissues were cut into approximately 1-2 mm^3 fragments using ophthalmic scissors and placed into 10 ml of digestive solution containing D-Hanks (Sigma), collagenase I (10 mg; Worthington, USA), DNase I (500 u Sigma), hyaluronidase (5 mg; Sigma), 2% fetal bovine serum (FBS; Gibco, USA), penicillin (100 u/ml; Sigma), and streptomycin (100 u/ml; Sigma). The digestion was performed at 37°C for 60 minutes on a constant temperature shaker and terminated with 20% FBS. The resulting cell suspension was filtered through a 40-μm disposable nylon strainer to remove debris. Cells were collected, washed with PBS, centrifuged, and resuspended. Red blood cells were lysed using erythrocyte lysis buffer (Beyotime, China) for 1 min at 4°C, followed by washing with PBS and centrifugation. The cell suspension was then gently layered onto Percoll (Baiaolaibo Technology Co. Beijing, China) separation medium and centrifuged. The mononuclear cells (MNCs) layer was carefully aspirated, washed with PBS, centrifuged, and resuspend for subsequent analysis. The MNCs were used for intracellular staining at room temperature for 30 minutes with the following antibodies diluted in 0.3% saponin (Sigma)/1% bovine serum albumin (BSA) (Sigma)-PBS buffer: the macrophage marker Alexa Fluor 488-ant-F4/80 (Bio-Rad, Hercules CA, USA), the pro-inflammatory M1 macrophage subtype markers PE-interleukin (IL)-12 (Thermo Fisher Scientfc, Waltham, USA), and anti-inducible nitric oxide synthase (iNOS) (Enzo Life Sciences, Farmingdale, USA), followed by staining with the corresponding PE-conjugated secondary antibodies (1:200, Alexa Fluor 555, goat anti-rabbit; Molecular Probes, Eugene, USA) for iNOS. Cells were gated using forward and sideward scatter characteristics, and at least 10,000 events were recorded using flow cytometer (BD Biosciences, USA). BD Biosciences' CellQuest software was used to evaluate the data. The proportions of double-positive cells were determined using quadrant analysis.

Western blot assay

Lung tissues from the remaining five mice in each group were harvested and homogenized on ice using a micro-operated tissue homogenizer (Kimble Kontes, Vineland, USA) in lysis

buffer provided by a protein extraction kit (Millipore, Tullagreen Carrigtwohill, Cork, Ireland) supplemented with a protease inhibitor cocktail. The homogenates were centrifuged at 12,000 g for 20 minutes at 4°C, and protein concentrations were measured using a bicinchoninic acid (BCA) protein assay kit (Sangon Biotech, Shanghai, China). Equal amounts of protein (20 μg per lane) were separated by sodium dodecyl sulfate-polyacrylamide gel electrophoresis and transferred onto a nitrocellulose membrane (Millipore). The membranes were blocked with 5% non-fat milk at room temperature for 1 h and then incubated overnight at 4°C with primary antibodies: anti-toll like receptor 2 (TLR-2; 1:1000; Cell Signaling Technology, Boston, USA), anti-p-nuclear factor kappa B (p-NF-κB; 1:1000; Cell Signaling Technology), anti-glyceraldehyde-3-phosphate dehydrogenase (GAPDH; 1:10,000; Cell Signaling Technology), and anti-ribosomal protein S3 (RPS3; 1:1000; Abcam, Cambridge, UK). After washing Tris-buffered saline containing 0.1% Tween-20 (TBST) in the next day, the membranes were incubated with horseradish peroxidase-conjugated secondary antibodies (1:10,000; Cell Signaling Technology) for 2 hours at room temperature. Proteins were detected using a Chemiluminescence Kit (Solarbio, Beijing, China), and the bands were visualized with a Molecular Imager ChemiDoc XRS1 System (Bio-Rad).

Serum and BALF cytokine assays

Serum levels of IL-6 (PeproTech, Rocky Hill, USA), IL-1β (MultSciences, Hangzhou, China), monocyte chemoattractant protein-1 (MCP-1) (Wuhan Boster Biological Technology Co., Ltd., Wuhan, China), and tumor necrosis factor (TNF)-α (PeproTech) were measured in blood samples obtained from asthmatic mice by cardiac puncture. ELISA was performed on both serum and BALF supernatants in accordance with the kit manufacturer's instructions. The cytokine concentrations were computed from the standard curve and presented as the means of triplicate determinations in pg/mL.

Immunohistochemical (IHC) staining

Paraffin-embedded lung tissue sections were routinely deparaffinized, rehydrated, and subjected to antigen retrieval, followed by blocking with 1% BSA at room temperature for 30 minutes. After washing the slices with PBS, the sections were incubated with at 4°C with primary antibodies against p-NF-κB (Santa Cruz Biotechnology, Dallas, USA), TLR-2 (Santa Cruz Biotechnology) and RPS3 (Invitrogen, Carlsbad, USA). Then, the sections were washed with PBS and incubated with 50 μl of biotinylated secondary antibody (Invitrogen) at room temperature for 2 hours. After an additional wash with PBS, sections were developed using 100 μl of freshly prepared DAB (Invitrogen) solution for 5-10 minutes and examined under light microscope. The sections were then rinsed with tap water, counterstained with hematoxylin, dehydrated through a gradient alcohol series, cleared, and mounted with neutral resin. Negative controls were prepared by replacing the primary antibody with PBS. Brownish-yellow granular staining in lung tissues was considered indicative of positive protein expression. For each specimen, five randomly selected sections were analyzed using Image-Pro Plus 6.0. The relative protein expression levels of TLR-2, RPS3, and p-NF-κB were quantified as the average optical density value.

Lung tissue transcriptomic sequencing and clinical validation of key pathways

RNA extraction and transcriptome sequencing: On day 34, left lung tissues of the remaining five mice from each group were aseptically collected, snap-frozen in liquid nitrogen, and stored at -80°C until RNA extraction. Total RNA was extracted using TRIzol reagent (Invitrogen) according to the manufacturer's instructions. RNA concentration and purity were measured using a NanoDrop 2000 spectrophotometer (Thermo Fisher Scientific), while integrity was verified with an Agilent 2100 Bioanalyzer (Agilent Technologies). Samples with an RNA integrity number > 7.0 were used for library construction. Sequencing libraries were prepared employing the NEBNext® Ultra™ II Directional RNA Library Prep Kit (New England Biolabs) and subsequently sequenced on an Illumina Novaseq 6000 platform (Illumina) to generate 150-bp paired-end reads, yielding approximately 20 million clean reads per sample.

Bioinformatic analysis: Raw sequencing data were processed with fastp software to remove adapter sequences and low-quality reads, yielding high-quality clean reads. These clean reads were subsequently aligned to the mouse reference genome (GRCm39) using HISAT2.

Transcript abundance was quantified as fragments per kilobase of transcript per million mapped reads (FPKM) using StringTie. Differential gene expression analysis between the FI and NA groups was performed using the DESeq2 R package, with genes satisfying |fold change| > 1.5 and FDR-adjusted *P*-value < 0.05 considered significantly differentially expressed (DEGs). KEGG pathway enrichment analysis for these DEGs was conducted using the clusterProfiler R package, with a significance threshold of FDR < 0.05.

Clinical sample collection: To validate the clinical relevance of findings from the mouse model, samples of human peripheral blood were obtained. Thirty patients with NA were recruited from the Department of Respiratory and Critical Care Medicine, The study protocol was approved by the Medical Ethics Committee (MEC) of the First Affiliated Hospital of Shanxi Datong University (Approval No: KYYJ-2024-005).

Study participants: Thirty patients with neutrophilic asthma (NA) were recruited from the Department of Respiratory and Critical Care Medicine. Diagnosis was established according to the Global Initiative for Asthma (GINA) guidelines and confirmed by sputum induction analysis (sputum neutrophil percentage > 76%). Twenty age- and sex-matched healthy volunteers with no history of chronic respiratory diseases or active infections served as the healthy control (HC) group.

Exclusion criteria: Subjects with comorbid chronic obstructive pulmonary disease, bronchiectasis, or active respiratory infections were excluded from both groups.

Sample collection: From each participant, 5 mL of peripheral blood was drawn into a serum separation tube for subsequent protein analysis and a PAXgene Blood RNA Tube (PreAnalytiX) for RNA analysis.

The diagnosis was established according to the Global Initiative for Asthma (GINA) guidelines and sputum induction analysis, defined by a sputum neutrophil percentage (NEU%) > 76%. Twenty age- and sex-matched healthy volunteers were recruited as the control (HC) group. Subjects with chronic obstructive pulmonary disease, bronchiectasis, or active respiratory infections were excluded. For each participant, 5 mL of peripheral blood was collected into serum separation tubes for protein analysis and PAXgene Blood RNA Tubes (PreAnalytiX, Hombrechtikon, Switzerland) for RNA analysis.

RNA extraction and quantitative real-time PCR from human blood: Total RNA was extracted from whole blood samples collected in PAXgene tubes using the PAXgene Blood RNA Kit (PreAnalytiX) according to the manufacturer's protocol. cDNA was synthesized from 1 μg of total RNA using the PrimeScript RT reagent Kit featuring gDNA Eraser (Takara Bio). Quantitative real-time PCR (qPCR) was performed on a QuantStudio 6 Flex System (Applied Biosystems) using SYBR Premix Ex Taq II (Takara Bio). The primer sequences were as follows: S100A8 (F: 5'-ATGCCGTCTACAGGGATGAC-3', R: 5'-CCCACTTTTATCACCATCGC-3'); CXCL2 (F: 5'-AGGGAAAAGCTTGCCTGAAA-3', R: 5'-TCCTTCAGGAACAGCCACCA-3'); GAPDH (F: 5'-GGAGCGAGATCCCTCCAAAAT-3', R: 5'-GGCTGTTGTCATACTTCTCATGG-3'). Relative mRNA expression levels, presented as fold change relative to the healthy control (HC) group, were calculated using the $2^{-\Delta\Delta Ct}$ method.

Human serum S100A8/A9 levels analyzed using ELISA: Peripheral blood samples were collected into serum separation tubes, left to clot at room temperature for 30 min, and then centrifuged at 3,000 rpm for 10 min. The resultant supernatant (serum) was aliquoted and stored at -80°C until analysis. Serum concentrations of the S100A8/A9 heterodimer (Calprotectin) were measured using a commercial Human S100A8/A9 Heterodimer ELISA Kit (Hycult Biotech, Uden, Netherlands or equivalent) in strict accordance with the manufacturer's guidelines. Absorbance was measured at 450 nm using a microplate reader, and concentrations were derived from standard curve. Results were expressed in nanograms per milliliter (ng/mL).

Statistical analysis

Statistical analyses were performed using GraphPad Prism 9.0. Data were presented as mean ± standard error of the mean (SEM) unless otherwise specified. For animal studies, group comparisons were conducted using Student's t-test or one-way ANOVA, while AHR data were analyzed by two-way repeated measures ANOVA with Bonferroni post-test.

Table 1. Comparison of behavioral stress scores among experimental groups (scores, mean ± SEM)

Group	Day 21	Day 27	Day 34	Overall Mean Score
NA	7.811 ± 0.9	8.254 ± 0.7	8.541 ± 0.6	8.218 ± 0.5
DI	4.232 ± 0.8*	3.839 ± 0.6*	3.532 ± 0.7*	3.827 ± 0.6*
FI	3.512 ± 0.7*,#	3.109 ± 0.5*,#	2.872 ± 0.4*,#	3.133 ± 0.5*,#

Notes: NA group, neutrophilic asthma group; DI group, dexamethasone intervention group; FI group, Fasudil intervention group; *P < 0.05 vs. NA group; #P < 0.05 vs. DI group.

Table 2. Component analysis of behavioral symptoms (scores, mean ± SEM)

Group	Breathing Pattern	Behavioral Activity	Neurological Symptoms	Overall Condition
NA	2.721 ± 0.3	2.876 ± 0.2	1.827 ± 0.4	1.650 ± 0.3
DI	1.326 ± 0.4*	1.602 ± 0.3*	0.814 ± 0.2*	0.705 ± 0.2*
FI	1.038 ± 0.3*,#	1.055 ± 0.2*,#	0.639 ± 0.2*,#	0.517 ± 0.1*,#

Notes: NA group, neutrophilic asthma group; DI group, dexamethasone intervention group; FI group, Fasudil intervention group; *P < 0.01 vs. NA group; #P < 0.05 vs. DI group.

For human data, normality was assessed using the Shapiro-Wilk test. Normally distributed data were reported as mean ± SEM and compared using unpaired t-test, whereas non-normally distributed data were reported as median and IQR and were compared using the Mann-Whitney U test. To evaluate associations between continuous variables, Pearson correlation analysis was performed. Specifically, this method was used to assess the linear relationships of S100A8 mRNA levels and S100A8/A9 protein concentrations with sputum neutrophil percentage. Statistical significance was defined as a two-tailed $P < 0.05$ for all analyses.

Results

Quantification of behavioral stress responses

Behavioral assessments revealed significant differences in stress responses among the three groups (**Table 1**). Mice in the NA group showed pronounced stress responses throughout the observation period, whereas both intervention groups showed significant improvements in behavioral responses.

Analysis of behavioral scores demonstrated that Fasudil intervention resulted in comprehensive improvement across all measured parameters (**Table 2**). In specific, the FI group showed significantly lower scores for breathing pattern abnormalities and behavioral activity disturbances, compared to the DI group ($P < 0.05$). The quantitative assessment demonstrates that Fasudil effectively alleviates behavioral stress responses in NA mice, with superior efficacy compared to dexamethasone in improving respiratory distress and abnormal behaviors.

Fasudil ameliorated lung histopathological alterations in NA mice

Histopathological examination of lung tissue sections showed obvious pathological changes in the NA group, including thickened bronchial walls, extensive infiltration of inflammatory cells surrounding the bronchi and pulmonary blood vessels, airway epithelial damage, and disrupted tissue architecture. In contrast, lung tissue from mice in the FI and DI groups was relatively intact, with slightly thickened bronchial walls and reduced infiltration of inflammatory cells around the bronchi compared to the NA group. Limited infiltrations of neutrophils, eosinophils, and lymphocytes were observed in the submucosa and alveolar interstitium (**Figure 1A**). Semi-quantitative analysis of peribronchial inflammation revealed significantly lower inflammation scores in both the DI ($P < 0.05$) and FI group ($P < 0.001$) compared with the NA group, with an even pronounced decrease observed in the FI group compared to the DI group ($P < 0.05$) (**Figure 1B**).

As demonstrated in **Figure 1C**, **1D**, the FI group showed a significant reduction in bronchial wall thickness compared to both the NA group ($P < 0.001$) and the DI group ($P < 0.05$). Similarly, inflammatory cell infiltration was markedly suppressed in the FI group relative to the NA ($P < 0.001$) and DI groups ($P < 0.05$). These objective measurements substantiate our qualitative observations and semi-quantitative scoring, confirming that Fasudil not only alleviates inflammatory cell recruitment but also effectively mitigates structural alterations in the airways.

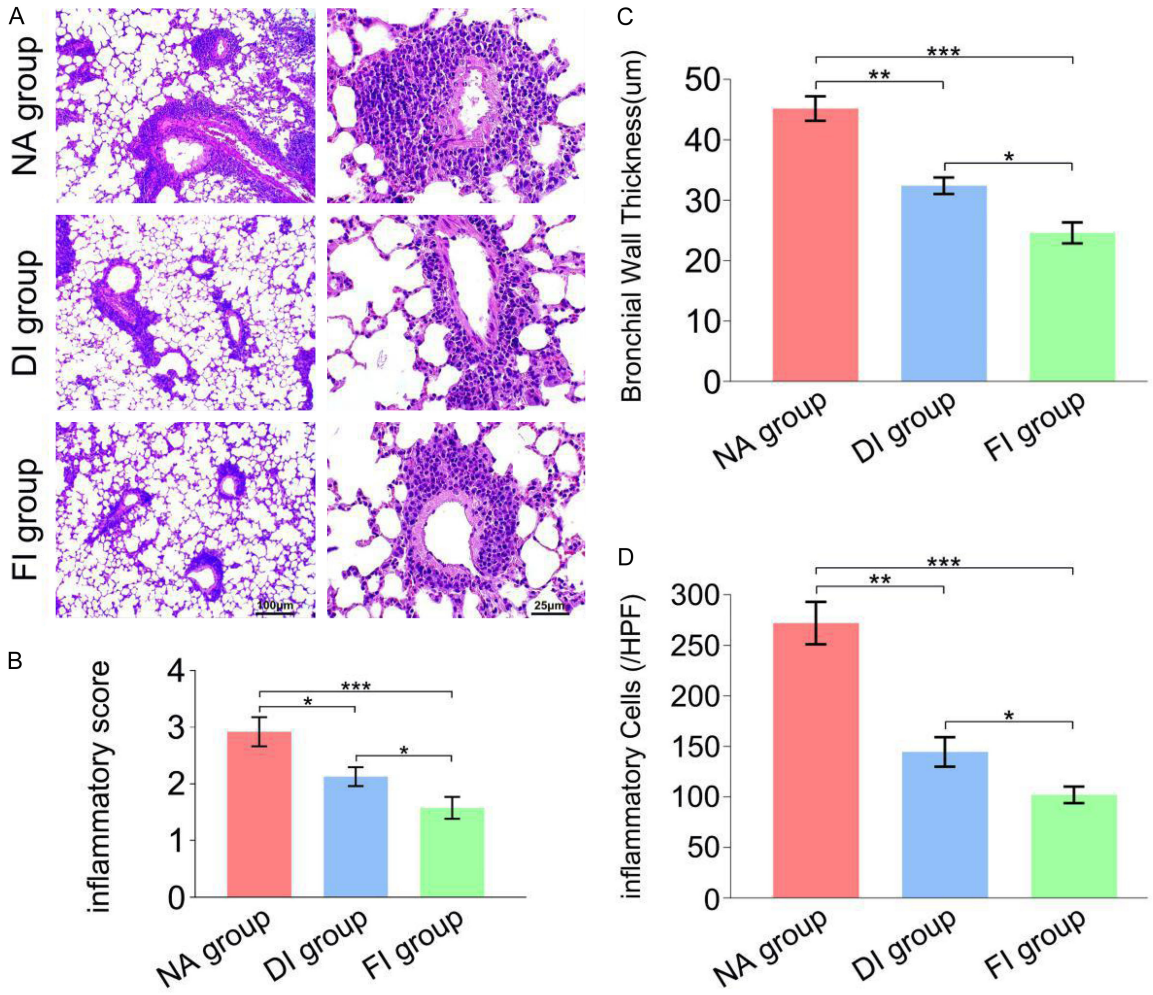

Figure 1. Fasudil alleviated pathological alterations and airway inflammation in neutrophilic asthma (NA) mice. A. Representative H&E-stained lung tissue sections. B. Semi-quantitative assessment of peribronchial inflammatory cell infiltration (scale: 0-4). C. Quantitative measurement of bronchial wall thickness (μm). D. Quantification of inflammatory cell count per high-power field (HPF, 400×). Notes: NA group, neutrophilic asthma group; DI group, dexamethasone intervention group; FI group, Fasudil intervention group; Data are presented as mean ± SEM (n = 5). *P < 0.05, **P < 0.01, ***P < 0.001.

Effects of Fasudil on BALF total cell counts and differential cell composition in NA mice

Analysis of BALF provided quantitative evidence of Fasudil's potent anti-inflammatory effects in NA. The cellular composition of BALF was markedly altered by both interventions, with Fasudil demonstrating superior efficacy in reducing overall cellularity and specific inflammatory cell populations. As shown in **Figure 2A**, the total cell count in BALF was dramatically elevated in the NA group, reflecting substantial inflammatory cell recruitment to the airways. Dexamethasone decreased the total cell count by approximately 39% compared with the NA group ($P < 0.05$), while Fasudil achieved a more pronounced reduction of approximately 55% ($P < 0.01$ vs. NA; $P < 0.05$ vs. DI).

Differential cell analysis revealed that Fasudil exerted particularly strong effect on neutrophil inflammation. Compared to the NA group, the NEU% in the DI and FI groups significantly decreased, with the FI group showing a notably greater reduction than the DI group ($P < 0.05$) (**Figure 2B**). Similarly, the Mφ% across all groups exhibited a dose-dependent decrease, with the FI group demonstrating significantly higher inhibition than the DI group ($P < 0.01$) (**Figure 2C**).

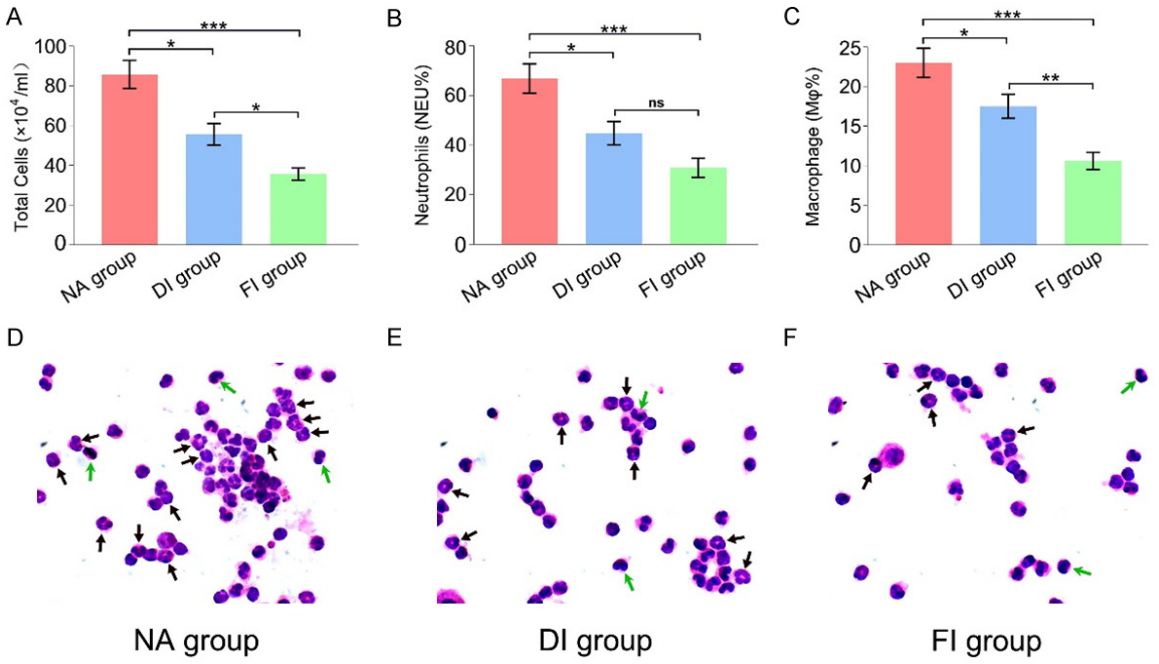

Figure 2. Fasudil altered the inflammatory cell profile in BALF. A. Total cell count (×10^4/mL); B. Percentage of neutrophils (NEU%); C. Percentage of macrophages (Mφ%); D-F. Representative cytospin images of BALF cells (Wright-Giemsa stain, 1000×), Green arrows indicate eosinophils; black arrows indicate neutrophils. Notes: NA group, neutrophilic asthma group; DI group, dexamethasone intervention group; FI group, Fasudil intervention group; BALF: bronchoalveolar lavage fluid; Data are presented as mean ± SEM (n = 5); *P < 0.05, **P < 0.01, ***P < 0.001, ns P > 0.05.

Representative cytospin preparations (**Figure 2D-F**) visually corroborated these quantitative findings. The NA group samples displayed dense cellular infiltration dominated by neutrophils (black arrows) and eosinophils (green arrows). Both treatment groups showed reduced cellularity, with the FI group exhibiting the most substantial clearance of inflammatory cells and restoration of normal cellular distribution.

Effects of Fasudil on cytokine levels in serum and BALF of NA mice

Analysis of serum cytokines revealed that, compared to the NA group, both the DI and FI groups exhibited significant reductions in MCP-1, IL-1β, TNF-α, and IL-6 levels (DI: $P < 0.05$, $P < 0.001$; FI: all $P < 0.001$). Furthermore, the FI group showed significantly lower levels of IL-6 and IL-1β than the DI group ($P < 0.05$, $P < 0.001$). Consistent trends were observed in BALF. Compared with the NA group, IL-6, IL-1β, and TNF-α levels were significantly reduced in the DI group ($P < 0.05$, $P < 0.01$, $P < 0.001$); in the FI group, MCP-1, IL-1β, TNF-α, and IL-6 levels were all significantly reduced ($P < 0.01$, $P < 0.001$). Furthermore, IL-1β in BALF was also significantly lower in the FI group than in the DI group ($P < 0.001$) (**Figure 3**).

Effects of Fasudil on macrophage polarization in NA mice

M1 macrophages are classically activated in NA and generally express high oxidative stress products and pro-inflammatory factors (e.g., iNOS and IL-12), causing inflammatory damage to tissues. Flow cytometry analysis showed that, compared with the NA group, the expression of iNOS and IL-12 in the lung tissue of both DI and FI groups were significantly reduced (DI group: $P < 0.05$, $P < 0.001$, respectively; FI group: $P < 0.01$, $P < 0.001$, respectively). Furthermore, compared with the DI group, there was a further reduction in IL-12 expression in the FI group ($P < 0.05$), whereas no significant difference was observed in iNOS expression between the two intervention groups (**Figure 4**).

Effects of Fasudil on the expression of RPS3, TLR-2 and p-NF-κB proteins in NA mice

IHC staining and western blot analyses were performed to evaluate the expressions of

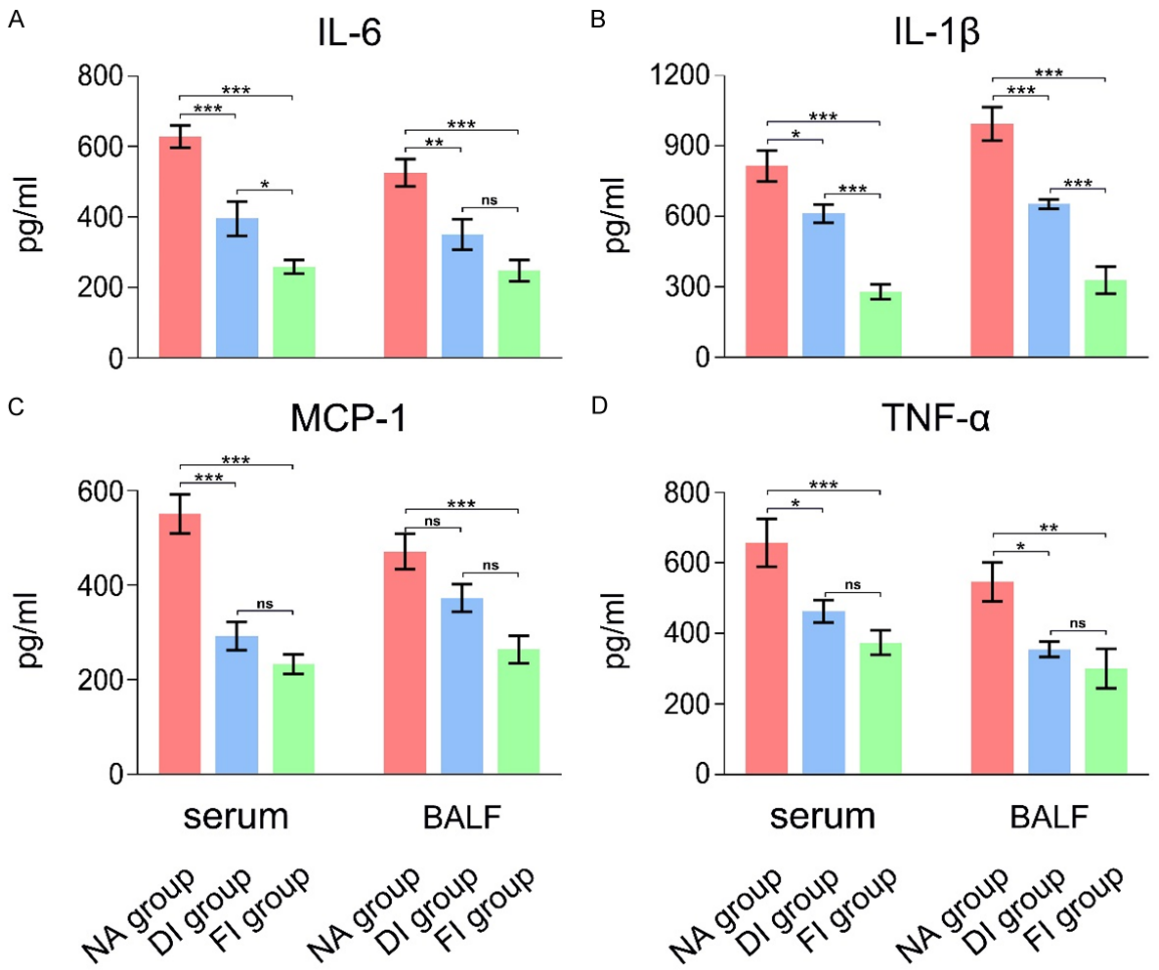

Figure 3. Fasudil suppressed cytokine levels in serum and BALF of NA mice. A. Interleukin (IL)-6; B. IL-1β; C. Monocyte chemoattractant protein-1 (MCP-1); D. Tumor necrosis factor (TNF)-α. Notes: NA group, neutrophilic asthma group; DI group, dexamethasone intervention group; FI group, Fasudil intervention group; BALF: bronchoalveolar lavage fluid; NA: neutrophilic asthma; Data are presented as mean ± SEM (n = 5); *P < 0.05, **P < 0.01, ***P < 0.001, ns P > 0.05.

RPS3, TLR-2, and p-NF-κB in the lung tissues. IHC staining demonstrated that RPS3, TLR-2, and p-NF-κB were highly expressed in the NA group. Compared with the NA group, the expression of p-NF-κB ($P < 0.05$) and TLR-2 ($P < 0.05$) was considerably lower in the DI group; similarly, the FI group exhibited significantly lower expression levels of RPS3 ($P < 0.001$), TLR-2 ($P < 0.01$), and p-NF-κB ($P < 0.01$). Specifically, Fasudil achieved a significantly greater reduction in the expression of p-NF-κB ($P < 0.05$) and RPS3 ($P < 0.05$) than dexamethasone (**Figure 5A**).

Consistent with the IHC findings, WB results also showed that the protein expression levels of p-NF-κB ($P < 0.001$), TLR-2 ($P < 0.001$) and RPS3 ($P < 0.05$) were significantly decreased in the FI group compared with the NA group; moreover, the FI group exhibited significantly lower levels of p-NF-κB ($P < 0.05$) and TLR-2 ($P < 0.05$) compared with the DI group (**Figure 5B**).

Fasudil ameliorated AHR and suppressed neutrophilic inflammation in a time-dependent manner

As shown in **Figure 6**, mice in the NA group exhibited severe AHR to increasing concentrations of MCh, which persisted from day 21 to day 34 (**Figure 6A**, **6C**, **6E**). However, Fasudil significantly attenuated AHR at all time points. Notably, compared to the NA group, the FI group already showed a rightward shift in the MCh

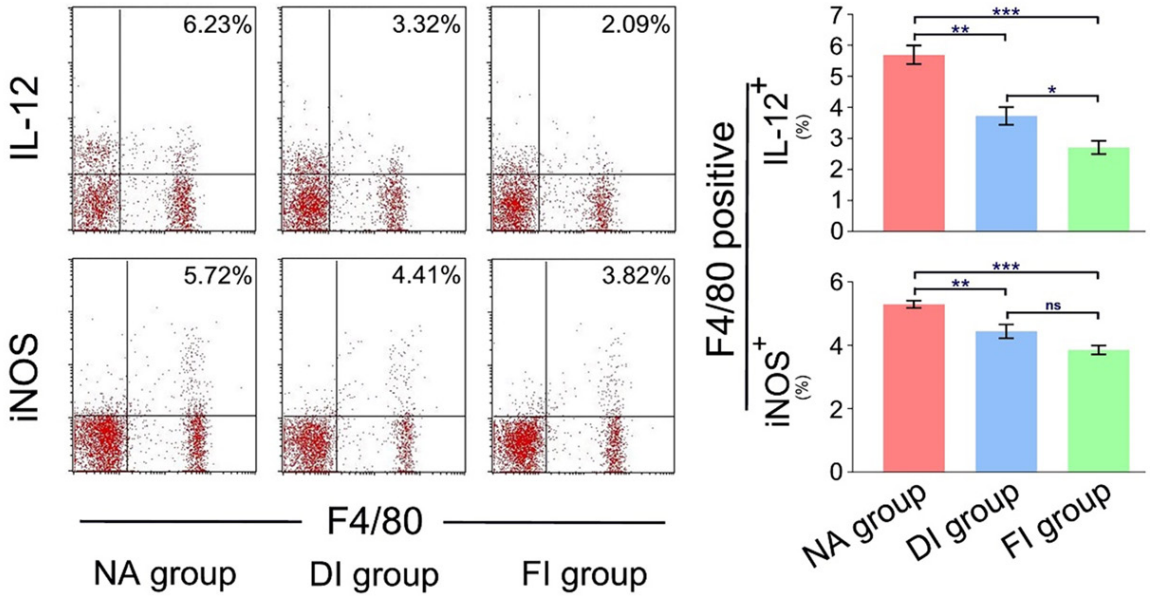

Figure 4. Fasudil modulated macrophages polarization in NA mice. Cells were stained with the macrophage marker Alexa Fluor 488-ant-F4/80, and the M1 macrophage subtype markers, including PE-IL-12, anti-inducible nitric oxide synthase (iNOS), were analyzed using flow cytometry. Results are shown as four-quadrant dot plots, with data expressed as the percentage of double-positive cells. Notes: NA group, neutrophilic asthma group; DI group, dexamethasone intervention group; FI group, Fasudil intervention group; NA: neutrophilic asthma; Data are presented as mean ± SEM (n = 5). *P < 0.05, **P < 0.01, ***P < 0.001, ns P > 0.05.

dose-response curve and reduced maximal Penh values on day 21 (P < 0.05), indicating a rapid onset of action (**Figure 6A**). This protective effect continued and became more pronounced at days 27 and 34, with significantly lower AHR in the FI group across nearly all MCh concentrations compared to the NA group (P < 0.001) (**Figure 6C**, **6E**). Dexamethasone also attenuated AHR, but its effect at day 21 was less pronounced than that of Fasudil, and at high MCh concentrations, the DI group showed higher Penh values at day 34 than the FI group (P < 0.05) (**Figure 6E**).

Consistent with the AHR results, analysis of BALF revealed a time-dependent suppression of neutrophilic inflammation by Fasudil (**Figure 6B**, **6D**, **6F**). The NEU% in BALF was higher in the NA group on days 21, 27, and 34. Compared with the NA group, the NEU% in the FI group began to decrease on day 21 (P < 0.05), with progressively greater decreases observed on day 27 (P < 0.01) and day 34 (P < 0.001) (**Figure 6F**). Although dexamethasone treatment also reduced NEU%, the FI group exhibited significantly lower NEU% than the DI group on days 27 and 34 (P < 0.05) (**Figure 6D**, **6F**). These data collectively indicate that Fasudil not only rapidly alleviates AHR but also progressively and potently suppresses neutrophilic airway inflammation over time, exhibiting a sustained therapeutic efficacy.

Transcriptomic profiling reveals Fasudil's mechanism of action and key biomarkers validated in clinical samples

Transcriptome sequencing of lung tissues revealed distinct gene expression profiles among NA, DI, and FI groups (**Figure 7A**). Compared to the NA group, Fasudil treatment resulted in 1,247 DEGs, including 652 downregulated and 595 upregulated genes (**Figure 7B**). KEGG enrichment analysis of the downregulated DEGs identified significant suppression of RhoA/ROCK signaling, NF-κB pathway, Toll-like receptor signaling, and neutrophil extracellular trap formation (**Figure 7C**). Key hub genes including Rock2, S100a8, S100a9, Mmp9, and Cxcl2 were identified as potential mediators of Fasudil's anti-inflammatory effects (**Figure 7D**).

Clinical validation demonstrated elevated expression of S100A8 (4.5-fold, P < 0.001) and CXCL2 (3.2-fold, P < 0.01) in NA patients versus healthy controls (**Figure 7E**). Serum calprotec-

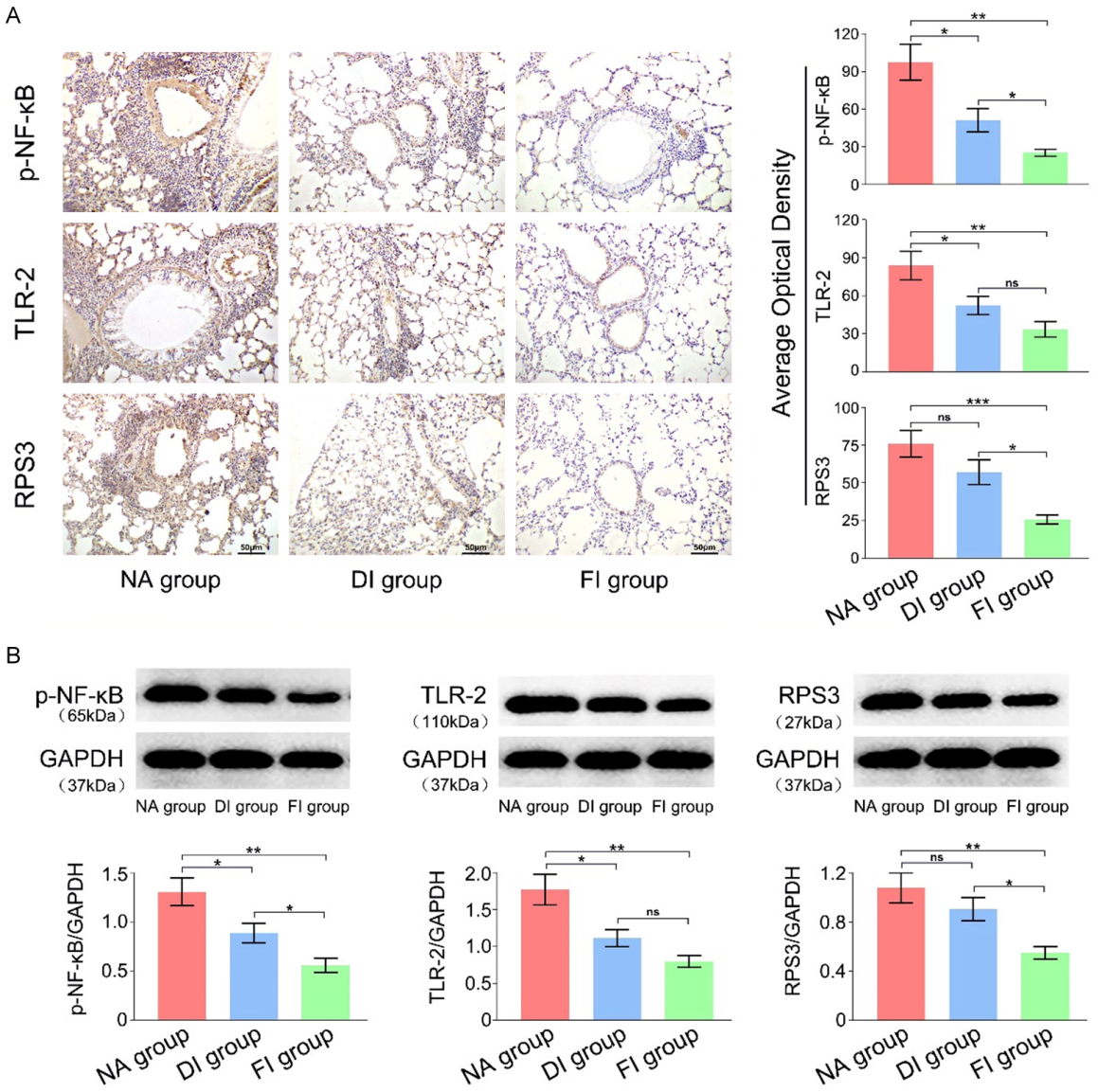

Figure 5. Fasudil reduced the expression of RPS3, TLR-2 and p-NF-κB proteins in NA mice. A. Left: Typical immunohistochemistry staining of lung tissues showing the expression of TLR-2, RPS3, and p-NF-κB. Brown-yellow granular deposits indicate positive staining (scale bar = 50 μm). Right: Quantification of the positive staining. B. Protein levels of TLR-2 (110 kDa), RPS3 (27 kDa), and p-NF-κB (65 kDa) as determined by western blot analysis. Notes: NA group, neutrophilic asthma group; DI group, dexamethasone intervention group; FI group, Fasudil intervention group; NA: neutrophilic asthma; Data are presented as mean ± SEM (n = 5). *P < 0.05, **P < 0.01, ***P < 0.001, ns P > 0.05.

tin (S100A8/A9) levels were also significantly increased in patients (P < 0.001) (**Figure 7F**). Both S100A8 mRNA and S100A8/A9 protein levels positively correlated with sputum neutrophil percentage (r = 0.72, P < 0.001; r = 0.65, P < 0.001) (**Figure 7G**), confirming their clinical relevance. These findings demonstrate that Fasudil exerts its therapeutic effects through coordinated inhibition of the RhoA/ROCK pathway and downstream inflammatory networks.

Discussion

The pathogenesis of asthma are traditionally attributed to eosinophilic inflammation and IgE-mediated mast cell degranulation. However, accumulating evidence underscores that neutrophils play a critical role in severe and steroid-resistant asthma phenotypes [19-21]. Post-mortem analyses have demonstrated a higher neutrophil burden in the lungs of fatal asthma

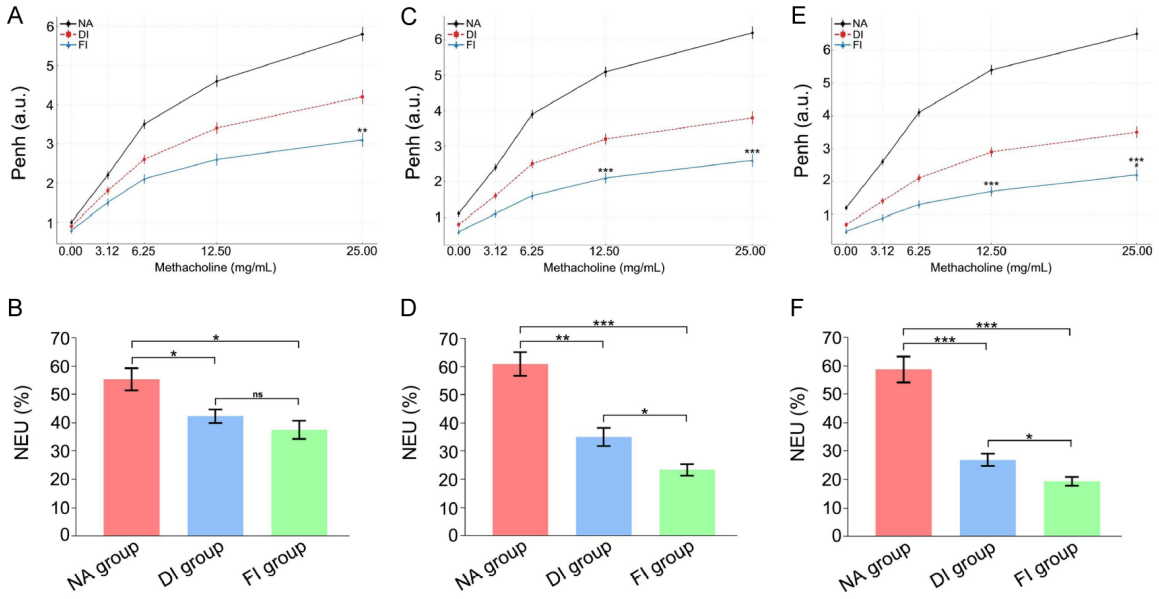

Figure 6. Time-course evaluation of airway hyperresponsiveness (AHR) and neutrophilic inflammation after Fasudil intervention. (A, C, E) Airway responsiveness measured by Enhanced Pause (Penh) upon exposure to escalating doses of methacholine (MCh) on day 21 (A), day 27 (C), and day 34 (E) days after the onset of OVA challenge. **P < 0.01, ***P < 0.001. (B, D, F) NEU% in BALF obtained immediately after lung function measurement on day 21 (B), day 27 (D), and day 34 (F). Notes: NA group, neutrophilic asthma group; DI group, dexamethasone intervention group; FI group, Fasudil intervention group; NA: neutrophilic asthma; BALF: bronchoalveolar lavage fluid; Data are presented as mean ± SEM (n = 5). *P < 0.05, **P < 0.01, ***P < 0.001, ns P > 0.05.

cases, and sputum neutrophilia is frequently observed during both persistent and acute exacerbations in both adults and children [22]. Consistent with these clinical observations, our murine model of NA demonstrated substantial infiltration of neutrophils and other inflammatory cells surrounding the bronchioles, alongside a significant increase in total cell and neutrophil counts in the BALF. Notably, treatment with Fasudil effectively ameliorated asthma-related behavioral manifestations (e.g., restlessness, dyspnea) and suppressed neutrophil aggregation in the airways, thereby alleviating neutrophilic inflammation and modifying disease progression.

This study objectively assessed the severity of stress responses in NA mice and the therapeutic effects of Fasudil using a multi-dimensional behavioral scoring system encompassing respiratory patterns, behavioral activities, neurological manifestations, and overall status. The results suggest that Fasudil ameliorates stress related responses in asthma mice through a dual mechanism: (1) inhibiting the Rho kinase pathway to reduce airway inflammation and remodeling, thereby reducing AHR and alleviating stress-related respiratory abnormalities; (2) modulating hypothalamic-pituitary-adrenal axis activity or suppressing central nervous system inflammation to directly mitigate stress-related behavioral abnormalities [23]. In contrast, dexamethasone, a classical glucocorticoid, primarily improves airway inflammation through anti-inflammatory effects but has limited regulatory effects on neuro-stress pathways, which may explain its inferior performance compared to Fasudil in respiratory patterns and behavioral activities. This study is the first to demonstrate that Fasudil can time-dependently improve AHR and inhibit neutrophilic inflammation in NA mice, and its therapeutic effect is superior to that of the traditional glucocorticoid dexamethasone. Fasudil reduced the Penh value as early as day 21 and maintained this effect through day 34, whereas dexamethasone showed weaker early efficacy and inferior anti-inflammatory effects at later stages. Given that NA represents a glucocorticoid-resistant and refractory asthma characterized by neutrophil-dominated airway inflammation, the rapid onset and sustained anti-inflammatory properties of Fasudil precisely compensate for the shortcomings of conventional glucocorticoid in treating NA.

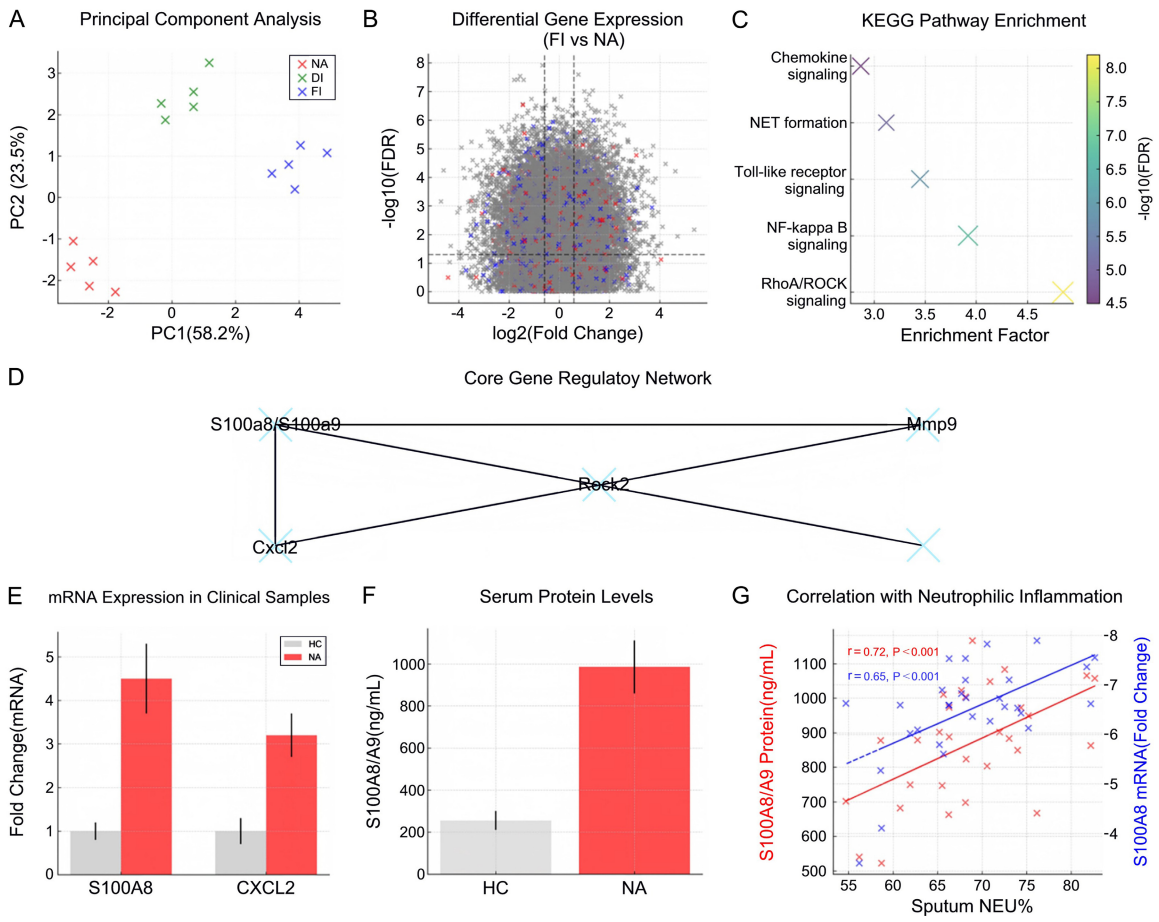

Figure 7. Transcriptomic analysis of Fasudil's mechanism and clinical validation of key biomarkers. A. Principal Component Analysis (PCA) plot of lung tissue transcriptomes from NA, DI, and FI groups, showing clear separation. B. Volcano plot of differentially expressed genes (DEGs) between the FI and NA groups. Significantly downregulated genes (FDR < 0.05, Log2FC < 0) are shown in blue, upregulated genes (FDR < 0.05, Log2FC > 0) in red, and non-significant genes in grey. Key downregulated genes are labeled. C. Bubble chart of KEGG pathway enrichment analysis for genes downregulated in the FI group. The size of the bubble represents the number of genes, and the color represents the -log10(FDR) value. D. A proposed network diagram illustrating core pathways and hub genes (e.g., Rock2, *S100a8/a9*, Mmp9, Cxcl2, Nfkb1) downregulated by Fasudil, centered around the inhibition of RhoA/ROCK signaling. E. mRNA expression levels of S100A8 and CXCL2 in peripheral blood from healthy controls (HC, n = 20) and neutrophilic asthma patients (NA, n = 30), presented as fold change relative to HC. F. Serum concentrations of S100A8/A9 (Calprotectin) in HC (n = 20) and NA (n = 30) groups. G. Correlation analysis between sputum neutrophil percentage (NEU%) and serum S100A8/A9 protein levels (left panel, n = 30) or blood S100A8 mRNA expression (right panel, n = 30) in NA patients. Notes: NA: neutrophilic asthma; Data are expressed as mean ± SEM.

We next investigated the underlying mechanisms, focusing on the interplay between macrophages and key inflammatory signaling pathways. Macrophage polarization is a hallmark of immune regulation [24]. In NA, classically activated M1 macrophages, induced by stimuli such as IFN-γ, LPS, or TNF-α [25, 26], are major contributors to disease pathology. These cells facilitate sustained neutrophil recruitment, activate Th1/Th17 responses, and promote airway remodeling and AHR through the secretion of pro-inflammatory factors [27]. Our data aligns with this paradigm: flow cytometry revealed elevated M1 markers (iNOS, IL-12) in asthmatic lungs, and ELISA confirmed high levels of M1-associated cytokines (MCP-1, IL-1β, TNF-α, IL-6) in serum and BALF. Critically, Fasudil treatment inhibited M1 polarization, as evidenced by reduced proportions of F4/80+iNOS+ and F4/80+IL-12+ cells, and concurrently suppressed the aforementioned cytokine cascade. Given that M1-derived factors like TNF-α and IL-1β directly drive airway smooth muscle hyperreactivity - a cornerstone of AHR - our results

indicate that Fasudil ameliorates neutrophilic airway inflammation, at least in part, by modulating M1 macrophage activity and its downstream effectors.

The pro-inflammatory functions of M1 macrophages are intrinsically linked to the activation of specific signaling hubs. Among these, NF-κB serves as a master regulator [28, 29]. Its phosphorylated form (p-NF-κB) initiates a pervasive inflammatory cascade, recruiting neutrophils and inducing mass production of cytokines, thereby creating a self-amplifying "inflammatory cycle" that sustains chronic inflammation [30, 31]. Furthermore, p-NF-κB promotes airway remodeling by regulating processes like cell proliferation and the release of tissue-destructive enzymes from neutrophils. Its role is amplified through crosstalk with other pathways, including MAPK, PI3K/Akt, and STAT6 [32].

This inflammatory network is further modulated by upstream pattern-recognition receptors and co-regulatory molecules. TLR-2, a pattern recognition receptor of the innate immune system, drives a vicious "inflammation-contraction-remodeling" cycle in NA. Activation of TLR-2 initiates downstream inflammatory cascades, while pro-inflammatory cytokines such as TNF-α and IL-1β enhance this process by augmenting airway smooth muscle contractility and AHR, largely through MAPK pathway [33-35]. Simultaneously, RPS3 functions as a critical non-ribosomal modulator of NF-κB. By directly interacting with the p65 subunit, RPS3 stabilizes the NF-κB complex on DNA, potentiating the transcription of neutrophil-chemoattractant mediators like TNF-α. Moreover, RPS3-mediated suppression of SIRT1 can trigger NLRP3 inflammasome activation and IL-1β release, adding another layer to the inflammatory response [36, 37].

Our findings position Fasudil within this regulatory framework. ICH demonstrated markedly elevated levels of p-NF-κB, TLR-2, and RPS3 in the NA group, which were potently suppressed by Fasudil. This suggests that the therapeutic benefits of Fasudil are mediated, at least in part, through the coordinated downregulation of this signaling axis. Notably, while dexamethasone also showed anti-inflammatory effects, Fasudil demonstrated a superior and more comprehensive modulatory profile. It was significantly more effective in reducing BALF macrophage infiltration, suppressing key pro-inflammatory cytokines (IL-6, IL-1β, TNF-α), and downregulating p-NF-κB and RPS3. This multi-targeted action, concurrently attenuating inflammmation and pathways linked to airway remodeling, may underlie Fasudil's enhanced efficacy and presents a promising therapeutic strategy.

This study further analyzed the molecular network of Fasudil through a combination of animal experiments and clinical sample verification, using transcriptome sequencing and bioinformatics analysis. Fasudil induced extensive alterations in gene expression profiles, with 652 genes significantly down regulated. KEGG pathway enrichment analysis revealed that Fasudil inhibited multiple key pro-inflammatory pathways, including RhoA/ROCK signaling, NF-κB activation, TLR signaling, and the formation of neutrophil extracellular traps. This multi-path inhibitory effect likely constitutes the molecular basis of Fasudil's powerful anti-inflammatory effects. In addition, the identification of core hub genes including ROCK2, S100A8, S100A9, Mmp9 and CXCL2, also provides mechanistic insight into Fasudil's anti-inflammatory action: these genes are involved in neutrophil activation, chemotaxis, and tissue remodeling processes. Fasudil significantly downregulates the expression of S100A8, S100A9, and CXCL2 in model mice. Combined with the high expression characteristics of these molecules in clinical samples, it further supports that Fasudil may improve the pathological process of neutrophil asthma by targeting these key molecules. These findings provide new ideas for the precise treatment and biomarker development of NA, laying a theoretical foundation for subsequent clinical translational research [38].

Nevertheless, this study has limitations. The potential crosstalk between M1 macrophage polarization and the p-NF-κB/TLR-2/RPS3 pathway was not fully elucidated, and our mechanistic exploration remained primarily within the realm of immune inflammation. Future work will focus on delineating these interactions and investigating strategies to directly alleviate airway remodeling and smooth muscle contraction.

Conclusion

Fasudil demonstrates significant therapeutic effect on NA, alleviating clinical symptoms and pathological lung alterations. Mechanistically, Fasudil inhibits M1 macrophage polarization, downregulates the expression of p-NF-κB, TLR-2, and RPS3 proteins, and suppresses the secretion of pro-inflammatory cytokines, including IL-6, IL-1β, MCP-1, and TNF-α. In addition, S100A8/A9 and CXCL2 emerge as potential clinical biomarkers for NA. Through these actions, Fasudil reduces airway inflammation, improves remodeling, and attenuates AHR, achieving its anti-asthmatic effect.

Acknowledgements

This study was supported by the Department of Science and Technology in Shanxi Province (Grant No. 20210302124314).

Disclosure of conflict of interest

None.

Address correspondence to: Shang-De Guo, Institute of Respiratory and Occupational Diseases, Shanxi Datong University, Datong, Shanxi, China. E-mail: guoshangde@sxdtdx.edu.cn

References

[1] Miller RL, Grayson MH and Strothman K. Advances in asthma: New understandings of asthma's natural history, risk factors, underlying mechanisms, and clinical management. J Allergy Clin Immunol 2021; 148: 1430-1441.

[2] Cazzola M, Rogliani P, Ora J, Calzetta L and Matera MG. Asthma and comorbidities: recent advances. Pol Arch Intern Med 2022; 132: 16250.

[3] Armeftis C, Gratziou C, Siafakas N, Katsaounou P, Pana ZD and Bakakos P. An update on asthma diagnosis. J Asthma 2023; 60: 2104-2110.

[4] Yu Y, Cao W, Xiao Y, Wei J, Huang H, Li A, Zhao M, Hu L, Poonsiri C, Teerawattananon Y, Morton A and Guo P. Assessing the value of omalizumab for pediatric asthma in China: a multicriteria decision analysis. Healthcare (Basel) 2025; 13: 2385.

[5] Chung KF, Dixey P, Abubakar-Waziri H, Bhavsar P, Patel PH, Guo S and Ji Y. Characteristics, phenotypes, mechanisms and management of severe asthma. Chin Med J (Engl) 2022; 135: 1141-1155.

[6] Rajvanshi N, Kumar P and Goyal JP. Global initiative for asthma guidelines 2024: an update. Indian Pediatr 2024; 61: 781-786.

[7] Sharma V and Cowan DC. Obesity, inflammation, and severe asthma: an update. Curr Allergy Asthma Rep 2021; 21: 46.

[8] Pelaia C, Melhorn J, Hinks TS, Couillard S, Vatrella A, Pelaia G and Pavord ID. Type 2 severe asthma: pathophysiology and treatment with biologics. Expert Rev Respir Med 2024; 18: 485-498.

[9] van der Veen TA, de Groot LES and Melgert BN. The different faces of the macrophage in asthma. Curr Opin Pulm Med 2020; 26: 62-68.

[10] Allam VSRR, Pavlidis S, Liu G, Kermani NZ, Simpson J, To J, Donnelly S, Guo YK, Hansbro PM, Phipps S, Morand EF, Djukanovic R, Sterk P, Chung KF, Adcock I, Harris J and Sukkar MB. Macrophage migration inhibitory factor promotes glucocorticoid resistance of neutrophilic inflammation in a murine model of severe asthma. Thorax 2023; 78: 661-673.

[11] Shilovskiy IP, Kovchina VI, Timotievich ED, Nikolskii AA and Khaitov MR. Role and molecular mechanisms of alternative splicing of Th2-cytokines IL-4 and IL-5 in atopic bronchial asthma. Biochemistry (Mosc) 2023; 88: 1608-1621.

[12] Rahmawati SF, Te Velde M, Kerstjens HAM, Dömling ASS, Groves MR and Gosens R. Pharmacological rationale for targeting IL-17 in asthma. Front Allergy 2021; 2: 694514.

[13] Britt RD Jr, Ruwanpathirana A, Ford ML and Lewis BW. Macrophages orchestrate airway inflammation, remodeling, and resolution in asthma. Int J Mol Sci 2023; 24: 10451.

[14] Xia L, Wang X, Liu L, Fu J, Xiao W, Liang Q, Han X, Huang S, Sun L, Gao Y, Zhang C, Yang L, Wang L, Qian L and Zhou Y. lnc-BAZ2B promotes M2 macrophage activation and inflammation in children with asthma through stabilizing BAZ2B pre-mRNA. J Allergy Clin Immunol 2021; 147: 921-932, e929.

[15] Wang Y, Wang X, Liu W and Zhang L. Role of the Rho/ROCK signaling pathway in the protective effects of fasudil against acute lung injury in septic rats. Mol Med Rep 2018; 18: 4486-4498.

[16] Liu C, Guo S, Liu R, Guo M, Wang Q, Chai Z, Xiao B and Ma C. Fasudil-modified macrophages reduce inflammation and regulate the immune response in experimental autoimmune encephalomyelitis. Neural Regen Res 2024; 19: 671-679.

[17] Yasuda Y, Wang L, Chitano P and Seow CY. Rho-kinase inhibition of active force and passive tension in airway smooth muscle: a strategy for treating airway hyperresponsiveness in asthma. Biology (Basel) 2024; 13: 115.

[18] Ngo U, Shi Y, Woodruff P, Shokat K, DeGrado W, Jo H, Sheppard D and Sundaram AB. IL-13 and IL-17A activate β1 integrin through an NF-κB/Rho kinase/PIP5K1γ pathway to enhance force transmission in airway smooth muscle. Proc Natl Acad Sci U S A 2024; 121: e2401251121.
[19] Gereda JE, de Arruda-Chaves E, Larco J, Matos E and Runzer-Colmenares FM. Severe asthma: Pathophysiology, diagnosis, and treatment. Rev Alerg Mex 2024; 71: 114-127.
[20] Gu W, Huang C, Chen G, Kong W, Zhao L, Jie H and Zhen G. The role of extracellular traps released by neutrophils, eosinophils, and macrophages in asthma. Respir Res 2024; 25: 290.
[21] Yamasaki A, Okazaki R and Harada T. Neutrophils and asthma. Diagnostics (Basel) 2022; 12: 1175.
[22] Wan R, Srikaram P, Guntupalli V, Hu C, Chen Q and Gao P. Cellular senescence in asthma: from pathogenesis to therapeutic challenges. EBioMedicine 2023; 94: 104717.
[23] Franova S, Molitorisova M, Kalmanova L, Palencarova J, Joskova M, Smiesko L, Mazerik J and Sutovska M. The anti-asthmatic potential of Rho-kinase inhibitor hydroxyfasudil in the model of experimentally induced allergic airway inflammation. Eur J Pharmacol 2023; 938: 175450.
[24] Li Y, Yang T and Jiang B. Neutrophil and neutrophil extracellular trap involvement in neutrophilic asthma: a review. Medicine (Baltimore) 2024; 103: e39342.
[25] Chang C, Chen G, Wu W, Chen D, Chen S, Gao J, Feng Y and Zhen G. Exogenous IL-25 ameliorates airway neutrophilia via suppressing macrophage M1 polarization and the expression of IL-12 and IL-23 in asthma. Respir Res 2023; 24: 260.
[26] Kotrba J, Müller I, Pausder A, Hoffmann A, Camp B, Boehme JD, Müller AJ, Schreiber J, Bruder D, Kahlfuss S, Dudeck A and Stegemann-Koniszewski S. Innate players in Th2 and non-Th2 asthma: emerging roles for the epithelial cell, mast cell, and monocyte/macrophage network. Am J Physiol Cell Physiol 2024; 327: C1373-C1383.
[27] Abohassan M, Al Shahrani M, Alshahrani MY, Begum N, Radhakrishnan S and Rajagopalan P. FNF-12, a novel benzylidene-chromanone derivative, attenuates inflammatory response in in vitro and in vivo asthma models mediated by M2-related Th2 cytokines via MAPK and NF-kB signaling. Pharmacol Rep 2022; 74: 96-110.
[28] Wan R, Jiang J, Hu C, Chen X, Chen C, Zhao B, Hu X, Zheng Z and Li Y. Correction for: neutrophil extracellular traps amplify neutrophil recruitment and inflammation in neutrophilic asthma by stimulating the airway epithelial cells to activate the TLR4/ NF-κB pathway and secrete chemokines. Aging (Albany NY) 2024; 16: 7505-7506.
[29] Liu L, Zhou L, Wang L, Mao Z, Zheng P, Zhang F, Zhang H and Liu H. MUC1 attenuates neutrophilic airway inflammation in asthma by reducing NLRP3 inflammasome-mediated pyroptosis through the inhibition of the TLR4/MyD88/NF-κB pathway. Respir Res 2023; 24: 255.
[30] Bok SH, Jang HE, Kim KH and Park DH. Puriton attenuates the asthma severity in ovalbumin-induced murine model via balancing Th1/Th2 and inhibiting inflammation. PLoS One 2025; 20: e0322792.
[31] Lyu X, Liu J, Liu Z, Wu Y, Zhu P and Liu C. Anti-inflammatory effects of reticuline on the JAK2/STAT3/SOCS3 and p38 MAPK/NF-κB signaling pathway in a mouse model of obesity-associated asthma. Clin Respir J 2024; 18: e13729.
[32] Li R, Wang J, Zhu F, Li R, Liu B, Xu W, He G, Cao H, Wang Y and Yang J. HMGB1 regulates T helper 2 and T helper17 cell differentiation both directly and indirectly in asthmatic mice. Mol Immunol 2018; 97: 45-55.
[33] Tian C, Gao F, Li X and Li Z. Icariside II attenuates eosinophils-induced airway inflammation and remodeling via inactivation of NF-κB and STAT3 in an asthma mouse model. Exp Mol Pathol 2020; 113: 104373.
[34] Bansal A, Kooi C, Kalyanaraman K, Gill S, Thorne A, Chandramohan P, Necker-Brown A, Mostafa MM, Milani A, Leigh R and Newton R. Synergy between interleukin-1β, interferon-γ, and glucocorticoids to induce TLR2 expression involves NF-κB, STAT1, and the glucocorticoid receptor. Mol Pharmacol 2023; 105: 23-38.
[35] Dong J, Liao W, Peh HY, Chan TK, Tan WS, Li L, Yong A and Wong WS. Ribosomal protein S3 gene silencing protects against experimental allergic asthma. Br J Pharmacol 2017; 174: 540-552.
[36] Yang L, Wang L, Tang Q, Liu Y, Meng C, Sun S, Chong Y, Zhang Y and Feng F. Hsa_circ_0093884 bound to RNA-binding protein RPS3 ameliorates hepatocyte inflammation in anti-tuberculosis drug-induced liver injury by competitively activating SIRT1. Int Immunopharmacol 2022; 110: 109018.
[37] Li Y, Huang B, Yang H, Kan S, Yao Y, Liu X, Pu S, He G, Khan TM, Qi G, Zhou Z, Shu W and Chen M. Author correction: Iatexin deficiency in mice up-regulates inflammation and aggravates colitis through HECTD1/Rps3/NF-κB pathway. Sci Rep 2025; 15: 32565.
[38] Wang J, Xu J, Zhao X, Xie W, Wang H and Kong H. Fasudil inhibits neutrophil-endothelial cell interactions by regulating the expressions of GRP78 and BMPR2. Exp Cell Res 2018; 365: 97-105.